# Structure and Properties of High-Speed Melt-Spun Filaments of Poly(butylene Terephthalate)

SHIDA CHEN* and JOSEPH E. SPRUIELL,† *Materials Science and Engineering, University of Tennessee, Knoxville, Tennessee 37996-2200*

## Synopsis

Filaments of poly(butylene terephthalate) were prepared by melt spinning with take-up velocities in the range 1000–5600 m/min. Two polymers with different molecular weights were used (intrinsic viscosities of 0.75 and 1.0 dL/g). The filaments were characterized using measurements of density, birefringence, shrinkage, thermal properties (differential scanning calorimetry), crystal size, crystalline orientation and phases present (wide angle X-ray diffraction), and tensile mechanical properties. Filaments spun from the 0.75 IV polymer with a mass throughput of 6 g/min at 1000 m/min have essentially amorphous structures, while higher take-up velocities result in $\alpha$-form crystals or, at the highest take-up velocity, a mixture of $\alpha$-form and $\beta$-form crystals. Only $\alpha$-form crystals were detected in the higher IV polymer. Crystal size varied with crystallographic direction but generally increased as take-up velocity increased. At the lowest take-up velocities the filaments increased in length during thermal shrinkage measurements. With increasing take-up velocity the shrinkage became positive and continued to increase until reaching a maximum in the range of the highest spinning speeds. This behavior correlates with the variation of the orientation factors of the amorphous phase. A plateau was observed in stress versus strain curves corresponding to strain-induced transformation from $\alpha$-form to $\beta$-form crystals. The length of this plateau increased with increase of take-up velocity and the $\alpha$-form crystal content in the sample. Both morphology and physical properties varied with polymer molecular weight and melt spinning conditions.

## INTRODUCTION

Poly(butylene terephthalate) (PBT) is a polymer that has been used primarily as an engineering thermoplastic and as a component in certain blends and block copolymers. It has the advantage in certain applications, such as moldings, that it crystallizes faster than poly(ethylene terephthalate) while exhibiting desirable physical and mechanical properties that are similar to the latter polymer. PBT has also attracted attention as a fiber forming material because of its ability to be processed into filaments that have high resilience and dyeability. In the present paper we report a systematic investigation of the structure and tensile mechanical properties of PBT filaments prepared by high speed melt spinning.

Early research on PBT[1-12] discovered that it exists in two crystalline forms ($\alpha$-and $\beta$-forms) and focussed on the determination of their crystal structures, and the relationship of these forms to the mechanical properties of PBT fibers

*On leave from: Textile Academy, Ministry of Textile Industry, East Suburb, Beijing, China.
†To whom all correspondence should be directed

Journal of Applied Polymer Science, Vol. 33, 1427–1444 (1987)

CCC 0021-8995/87/041427-18$04.00

and films. Both forms have triclinic unit cells; the major difference between them is that the crystallographic repeat distance along the chain axis direction ($c$-axis) is longer in the $\beta$-form than in the $\alpha$-form (about 12.6 Å for $\beta$ as compared to about 11.8 Å for $\alpha$). This difference results because the conformation of the four methylene group sequence is more extended in the $\beta$-form than in the $\alpha$-form. The $\alpha$-form is normally present in slowly cooled or annealed samples, but, above a critical applied stress level, the $\alpha$-form can undergo a reversible strain induced transformation to the $\beta$-form. Extensive plastic deformation near room temperature can stabilize the $\beta$-form, and, hence, drawing and annealing conditions have a marked influence on the structure and mechanical properties of PBT fibers as was recently shown in a contribution from our laboratory.[13] In that study filaments were spun only at a take-up velocity of 700 m/min with the emphasis placed on subsequent drawing and annealing treatments. In the present investigation we examine the structure and tensile mechanical properties of PBT filaments prepared by spinning over a range of conditions including take-up velocities up to 5600 m/min. The effect of varying the molecular weight of the polymer was also examined.

## EXPERIMENTAL

### Materials

Two PBT resins were used; both were supplied by Celanese Plastics and Specialties Company and are sold under the trade name Celanex 2000. One resin had an intrinsic viscosity (IV) of 0.75 dL/g while the second resin had an IV of 1.0 dL/g. The chips were dried in a laboratory vacuum oven for 10 h at 120°C prior to extrusion.

### Melt Spinning

The filaments were spun using a screw extruder with a 13 mm diameter screw. The melt was metered to a monofilament spinneret by a gear pump. The single capillary die had a diameter of 0.762 mm and an $L/D$ ratio of 5.0. The mass throughput of the polymer was carefully adjusted and controlled by the gear pump at either 4.0 or 6.0 g/min. A pneumatic device (aspirator) supplied by Rhone Poulenc Fibres, Inc. was used to draw the filaments down. The take-up velocities of the as-spun filaments were adjusted by changing the pressure of the compressed air supplied to the drawdown device. Samples with take-up velocities in the range of 1000 to 5600 m/min could be readily prepared with this technique. Since no winding device was used, the samples collected for characterization were in a relaxed state rather than being wound on a bobbin at constant tension. The quoted take-up velocity was calculated from the measured mass throughput, final filament diameter and filament density.

### Sample Characterization

Sample densities were determined using a density gradient column prepared from aqueous solutions of sodium bromide. The measured density was used to

compute the weight fraction crystallinity $X_c$ from the relation

$$X_c = \frac{\rho - \rho_a}{\rho_c - \rho_a} \cdot \frac{\rho_c}{\rho} \tag{1}$$

where $\rho_c$, $\rho_a$, and $\rho$ are the theoretical crystalline density, amorphous density, and experimental sample density, respectively. The crystalline density was taken to be that of $\alpha$-form, 1.396 g/cm$^3$ [1] and the amorphous density was taken to be 1.281 g/cm$^3$.[13]

Wide angle X-ray diffraction (WAXS) photographs were made using a flat plate camera and a Philips Norelco X-ray generator operated at 30 kV and 20 mA. Nickel filtered CuK$\alpha$ radiation was used with an exposure time of 8 h.

Diffractometer scans used for X-ray crystallinity analysis and for crystallite size measurements based on diffraction peak breadths were obtained using a fully automated Rigaku Geigerflex diffractometer equipped with a graphite crystal diffracted beam monochromator set to obtain CuK$\alpha$ radiation. A sample rotating device was used during collection of data for crystallinity measurements in order to help eliminate the effects caused by sample orientation.

Separation of overlapping diffraction peaks and resolution of the crystalline and amorphous contributions to the diffraction pattern were carried out using a technique similar to that of Heuvel et al.[14] This technique involves curve fitting the intensity data to a series of peaks described mathematically by the Pearson VII function defined by

$$f(x) = \frac{I_0}{\left[1 + 4Z^2(2^{1/m} - 1)\right]^m} \tag{2}$$

where $Z = (x - x_0)/H$, $x$ is the angle $2\theta$, $x_0$ is the position of the center of the peak, $H$ is the half width of the peak, $I_0$ is the intensity at the center of the peak, and $m$ is the shape parameter of the peak.

Small angle X-ray scattering (SAXS) patterns were made using the special facilities of the National Center for Small Angle Scattering at the Oak Ridge National Laboratory. These facilities were used after exposure times proved to be excessive using a camera mounted on the same generator used for WAXS patterns.

Thermal analysis of the as-spun filaments were carried out using a Perkin-Elmer DSC-2 equipped with a microcomputer data station. Runs were made with temperature increasing at a rate of 10°C/min.

Crystalline orientation factors were measured using the Rigaku diffractometer equipped with a fiber goniometer and pinhole collimation. Step scans through the azimuthal angle were made with 1° increments. A PDP 11/34 minicomputer provided data acquisition and analysis. The intensity data for the 010 and 100 reflections were used to compute $\langle \cos^2 \Phi_{hkl,z} \rangle$ in each case. These values were used to compute the Hermans' orientation factor for the PBT crystals from the relation

$$f_c = 1 - \tfrac{3}{2}\left(\langle \cos^2 \Phi_{100,z} \rangle + \langle \cos^2 \Phi_{010,z} \rangle\right) \tag{3}$$

where $\Phi_{hkl,z}$ is the angle between the normal to the ($hkl$) planes and the fiber axis $z$. The derivation of eq. (3) is based on the assumption that a pseudoorthorhombic unit cell may be used to describe the PBT structure in a manner similar to that used for the case of PET.[15-17]

Birefringence measurements were made using a Leitz polarizing microscope equipped with a filar eyepiece and a 30 order Berek compensator.

Amorphous orientation factors were computed from the relation[18]

$$\Delta n = X_c \cdot \Delta_c^0 \cdot f_c + (1 - X_c) \cdot \Delta_a^0 \cdot f_a + \Delta n_{\text{form}} \tag{4}$$

where $\Delta n$ is the measured birefringence, $\Delta_c^0$ is the intrinsic birefringence of the crystalline phase, $\Delta_a^0$ is the intrinsic birefringence of the amorphous phase, and $f_a$ is the amorphous orientation factor. The form birefringence $\Delta n_{\text{form}}$ was neglected.

The shrinkage of the filaments was determined by measuring the change in length of 30 cm of each filament after immersion in boiling water for 8 min. A load of 1 g/den was applied during measurement of the length. Shrinkage was calculated from

$$\text{percent shrinkage} = \frac{L_0 - L}{L_0} \times 100 \tag{5}$$

where $L$ is the length of the filament after shrinkage and $L_0$ is the initial length.

Load vs. extension curves were carried out using an Instron testing machine located in a conditioned room at 20°C and 65% relative humidity. The gage length was 2.54 cm and the strain rate was adjusted so that the samples broke in 20 ± 3 s.

## RESULTS AND DISCUSSION

### Density and Crystallinity

Figure 1 shows that the density increased with increase of take-up velocity. At any given take-up velocity the magnitude of the density was also dependent on the mass throughput and the polymer molecular weight (IV). It is noteworthy that for the lower mass throughput of 4 g/min the filament density is higher for the lower IV polymer, but for the higher mass throughput of 6 g/min the density is higher for the higher IV polymer. The differences of behavior appear to be related to the interrelationship of crystallization kinetics, cooling rates, and spinline stress developed at the point where crystallization occurs in the spinline. We will return to this discussion after presenting additional data.

Figure 2 presents WAXS patterns for selected filaments. For the sample spun with a mass throughput of 6 g/min and a take-up velocity of 1000 m/min, the pattern exhibits a diffuse halo indicating that this sample is essentially amorphous. This is consistent with the low density of this sample as shown in Figure 1. As take-up velocity increases to about 1500 m/min, a broad diffraction arc indicative of the presence of crystallization is observed.

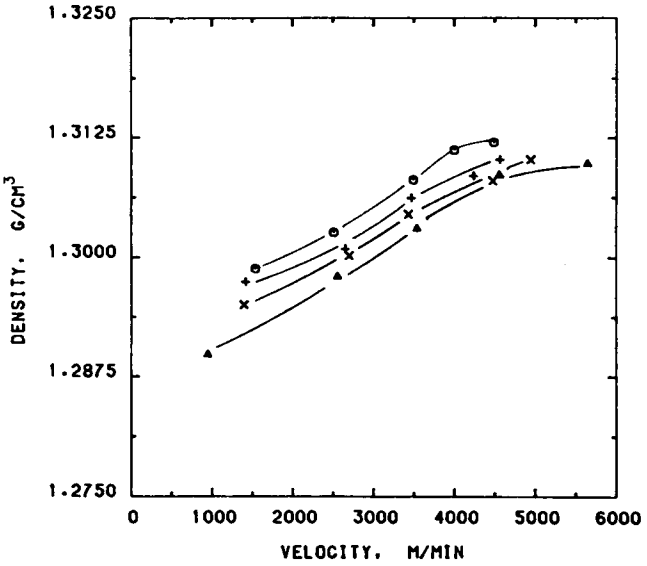


Fig. 1. As-spun filament density as a function of take-up velocity: (⊙) IV = 0.75, Q = 4 g/min; (+) IV = 1.0, Q = 4 g/min; (×) IV = 1.0, Q = 6 g/min; (▲) IV = 0.75, Q = 6 g/min.

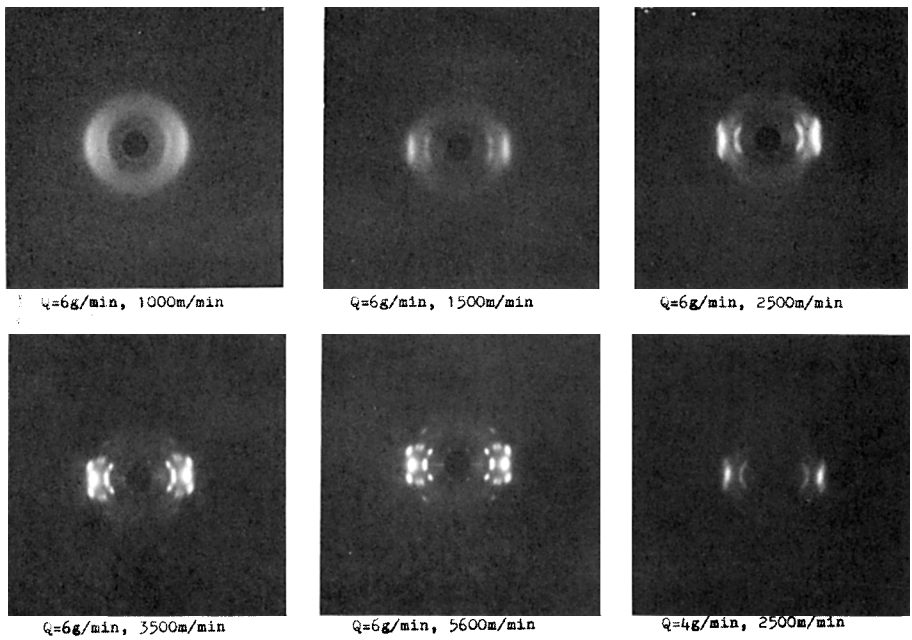


Fig. 2. X-ray fiber patterns for the as-spun filaments made at various take-up velocities.

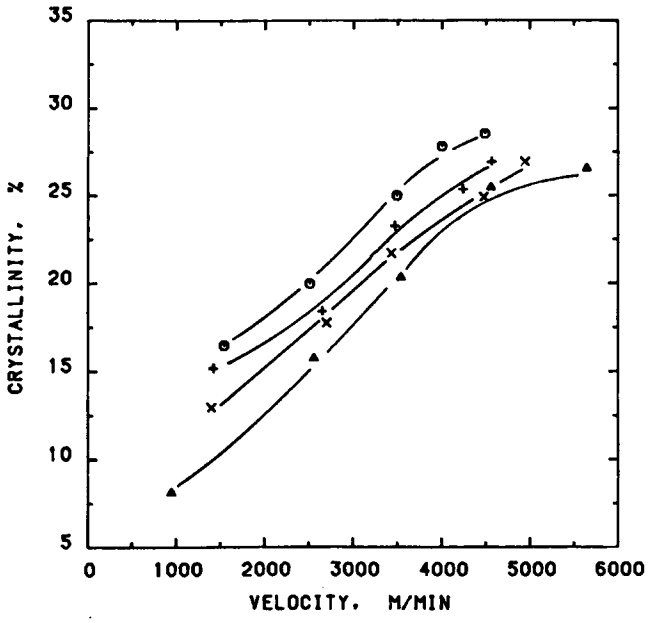


Fig. 3. As-spun filament crystallinity versus take-up velocity: (⊙) IV = 0.75, Q = 4 g/min; (+) IV = 1.0, Q = 4 g/min; (×) IV = 1.0, Q = 6 g/min; (▲) IV = 0.75, Q = 6 g/min.

Further increases in spinning speed or a decrease of mass throughput result in patterns with much sharper and more intense crystalline reflections. These changes are indicative of both increased crystallinity, increased crystallite size, and increased crystalline orientation.

Figure 3 presents the crystallinity values computed from the density data of Figure 1. The computation of these crystallinity values assumes that the crystals present are entirely of the $\alpha$-form, and the trends observed parallel those of the density data.

Let us now return to the discussion of possible reasons for the observed order of the crystallinity data shown in Figure 3. For a given polymer, a decrease of mass throughput should increase the cooling rate and spinline stress developed at any given take-up velocity. The increased cooling rate should decrease the crystallinity in the absence of a change in stress, but the increased level of stress should result in greater stress induced crystallization. In the present case, as well as for other polymers such as PET,[19,20] the effect of increased stress overrides the effect of increased cooling rate and the crystallinity increases with a decrease of mass throughput.

Increasing the molecular weight should increase the spinline stress, due to increased viscosity, without change of cooling rate. This effect should lead to an increase in stress induced crystallization. This is apparently the explanation why the crystallinity is higher for the higher IV sample when both samples are spun with a throughput of 6 g/min. In this case the spinline stress in the low IV polymer is so low at low spinning speeds that the sample barely crystallizes at all. The stress is sufficient for the higher IV polymer spun under these same conditions to produce a measurably greater level of crystallinity. Crystallization rates and ultimate crystallinities developed by

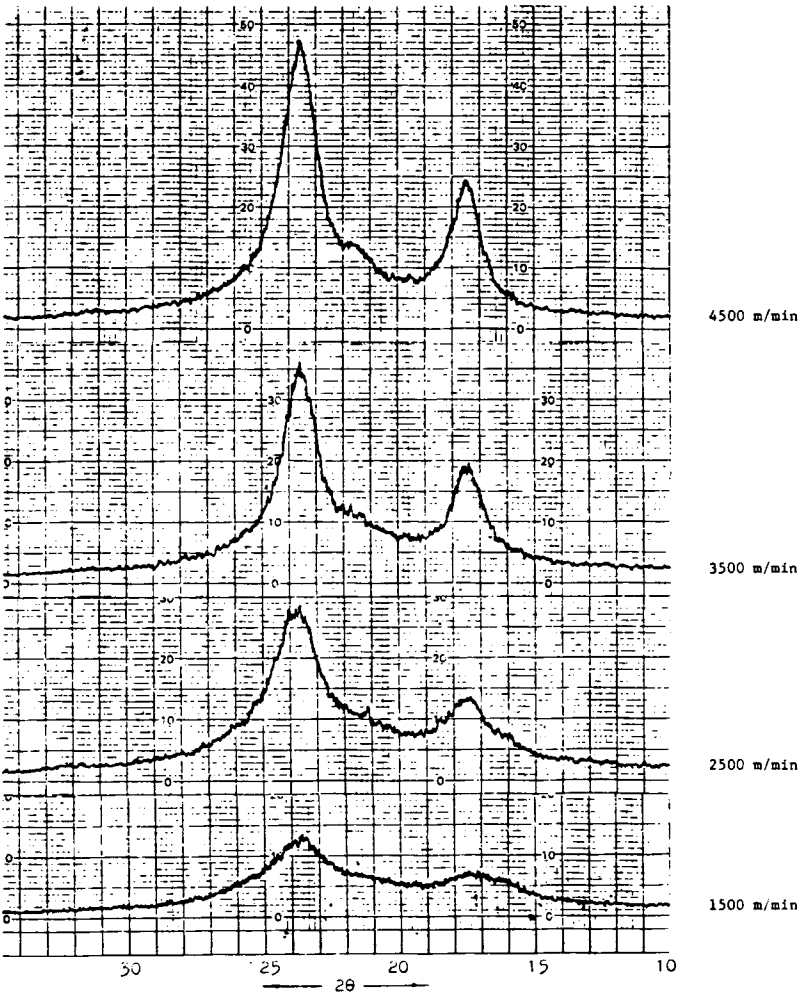


Fig. 4. Equatorial wide-angle X-ray diffraction patterns for as-spun filaments at the indicated take-up velocities: IV = 0.75, Q = 4 g/min.

polymers may also be independently affected by resin characteristics such as molecular weight. Higher molecular weight results in greater entanglements and lower chain segment mobilities. In the absence of stress and molecular orientation this normally results in reduced crystallization rates and lower ultimate crystallinities.[21,22] This effect appears to have influenced the results for the two polymers when spinning was carried out with a mass throughput of 4 g/min. In this case the balance of the effects of molecular weight and spinning stress is such that the lower IV polymer reaches the higher crystallinity level at each take-up velocity studied.

Equatorial scans for a few selected filaments are shown in Figure 4. These scans further illustrate the changes in the WAXS patterns. For filaments spun at low and medium take-up velocities, only the 010 and $1\bar{0}0$ reflections can be detected. But at the highest take-up velocities the $1\bar{1}0$ reflection is also observed.

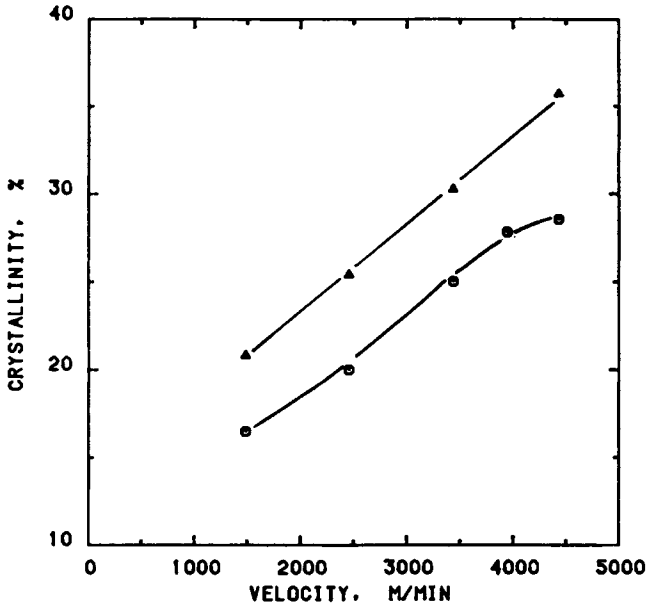


Fig. 5. Crystallinity vs. take-up velocity, IV = 0.75, Q = 4 g/min: (⊙) by density measurement; (▲) by X-ray measurement.

Figure 5 compares the crystallinity computed from the density data to that obtained by the X-ray diffraction technique for the case of the lower IV polymer spun with a throughput of 4 g/min. The dependence on take-up velocity is similar for the two measurements, though there is a slightly higher crystallinity indicated by the X-ray measurements. This difference is not surprising as it is well known that X-ray and density techniques give different crystallinity values due to the fact that each technique has its own set of assumptions and limitations. However, the fact that the X-ray results are significantly higher in the present case suggests an alternative interpretation that the samples contain a small amount of $\beta$-form that has nearly the same density as the amorphous phase. Since the two results also diverge slightly at the highest take-up velocities, this interpretation suggests that if $\beta$-form is present, its relative amount may increase slightly with increased take-up velocity.

## Crystal Form and Crystal Size

In order to examine the possibility that $\beta$-form is present we measured the position of the $\bar{1}04$ and $\bar{1}06$ reflections. For the $\alpha$-form these reflections should occur in meridional scans at $2\theta$ values of about 31.5° and 48.1°, while for the $\beta$-form they should occur at about 28.2° and 43.5°, respectively. In addition the $\bar{1}05$ for the $\alpha$-form occurs at about 39.4°. Figure 6 presents meridional scans for selected filaments. In all filaments there are peaks at $2\theta$ values of about 31° and 39°, indicating the predominence of $\alpha$-form in all samples. In the lower IV polymer, spun at the highest take-up velocities, there are also small but detectable peaks near $2\theta$ values of 43° and 28.2°, which means that

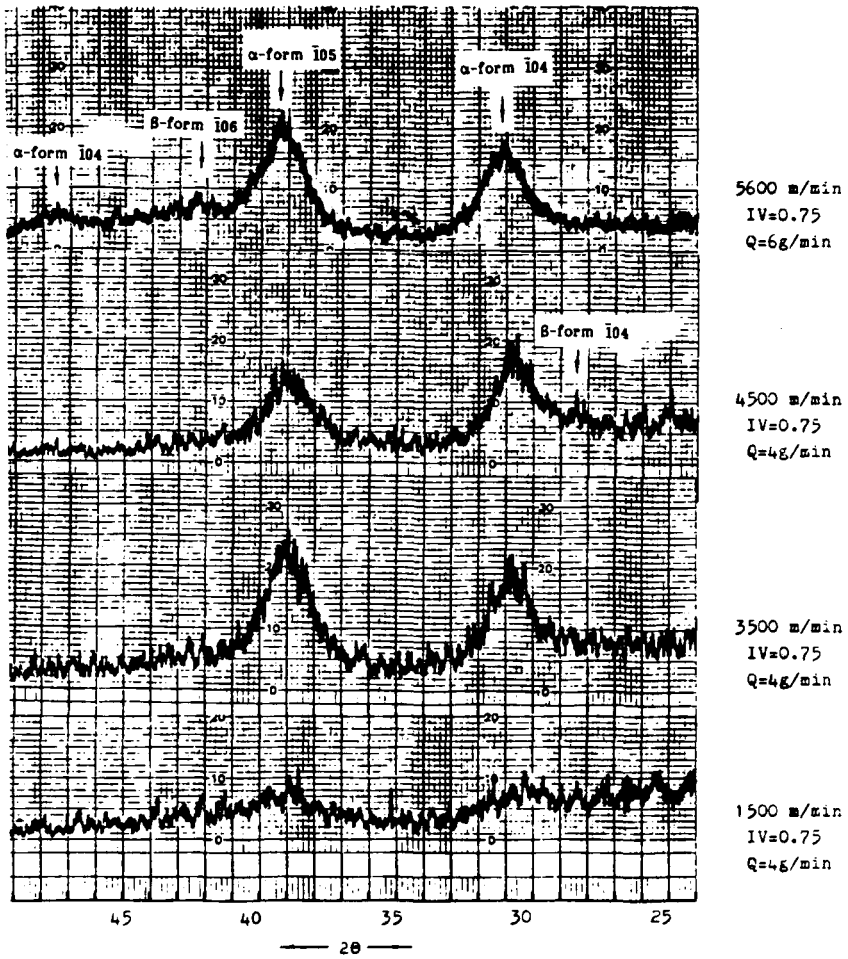


Fig. 6. Wide-angle X-ray meridional scanning pattern of selected filaments.

a small amount of $\beta$-form coexists with the $\alpha$-form in these samples. These results suggest that the crystallinity values computed from the filament densities are slightly low due to the presence of a small amount of $\beta$-form, and this error increases with increasing take-up velocity.

The actual length of the $c$-axis (chain crystallographic repeat) may be computed from the measured locations of the 104 reflection. These values and the lengths of the $a$- and $b$-axes are presented in Table I. Also presented in Table I are average crystal dimensions in directions perpendicular to the (010), (100), and ($\bar{1}04$) planes. These values were determined from the width at half maximum intensity of the reflections from these planes. In the case of the 010, 1$\bar{1}$0, and 100 reflections the peaks were resolved mathematically using the Pearson VII curve fitting procedure. It is observed that the crystal dimensions vary with direction; the dimension perpendicular to the (010) plane is the largest and the dimension perpendicular to the ($\bar{1}04$) plane which is near the chain axis direction is the smallest. It is especially to be noted that the crystal size increases with increase in the filament take-up velocity.

TABLE I
Results from Analysis of WAXD Patterns

| Velocity (m/min) | Unit cell (Å) | | | Apparent crystal size (Å) | | | Long period distance (Å) |
|---|---|---|---|---|---|---|---|
| | *a*-axis | *b*-axis | *c*-axis | $\Lambda^*100$ | $\Lambda^*010$ | $\Lambda^*\bar{1}04$ | |
| 1500 | 4.785 | 5.905 | 12.00 | 28 | 25 | 34 | 110 |
| 2500 | 4.765 | 5.895 | 11.97 | 38 | 47 | 42 | 110 |
| 3500 | 4.753 | 5.889 | 11.93 | 58 | 59 | 45 | 110 |
| 4500 | 4.745 | 5.878 | 11.84 | 62 | 69 | 60 | 123 |

DSC measurements of the melting peak temperature are presented in Figure 7. It is observed that the peak temperature increases with an increase of filament take-up velocity and reduction of mass throughput. These trends are evidently due to the change of crystal size already documented. The experimental melting temperature is shown as a function of crystal volume in Figure 8.

The SAXS patterns of the filaments were of the two-point type. The long period spacings computed from the SAXS patterns of selected filaments are also shown in Table I. These values are approximately constant at low and moderate take-up velocities, but they increase somewhat at the highest take-up velocities. It should also be pointed out that the intensities of the SAXS patterns were rather weak, which indicates only modest electron density differences in the samples.

## Molecular Orientation

The birefringence of the as-spun filaments is plotted in Figure 9 as a function of take-up velocity. The birefringence increases monotonically with

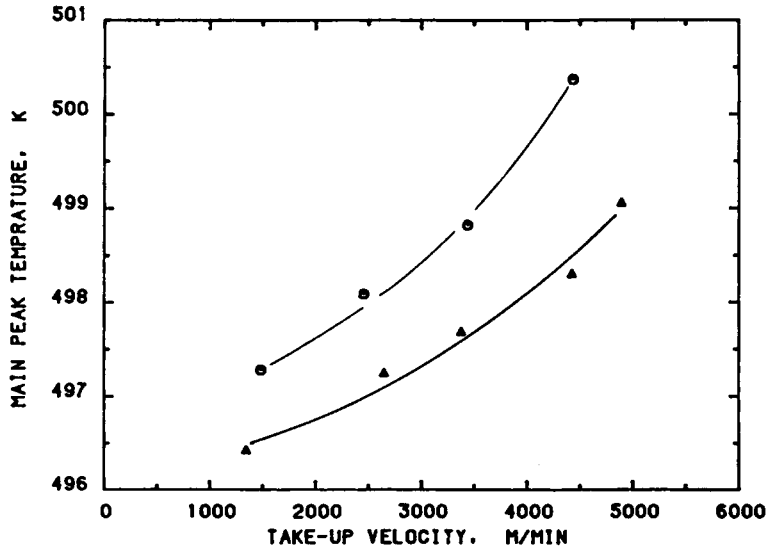


Fig. 7. Peak melting temperature in DSC curves dependence on take-up velocity: (⊙) IV = 0.75, Q = 4 g/min; (▲) IV = 1.0, Q = 6 g/min.

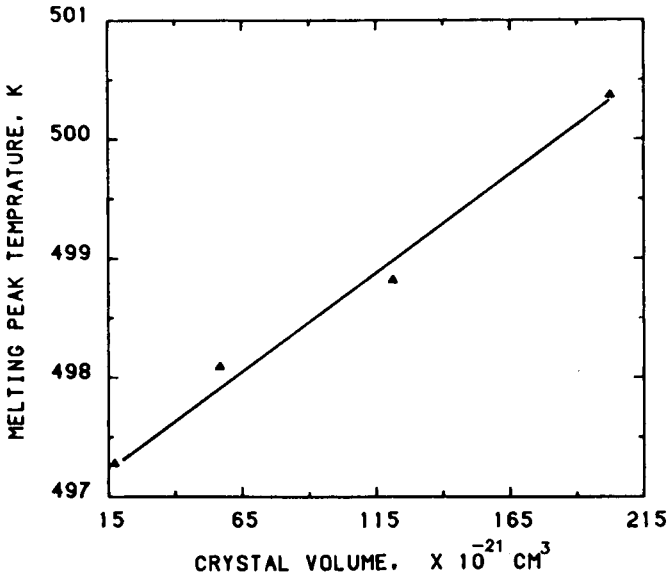


Fig. 8. Peak melting temperature in DSC curves vs. crystal volume.

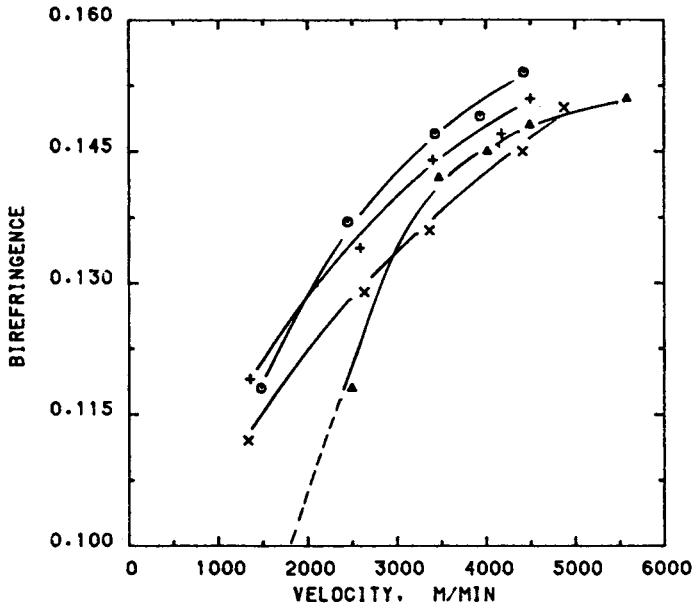


Fig. 9. Birefringence vs. take-up velocity: (⊙) IV = 0.75, Q = 4 g/min; (+) IV = 1.0, Q = 4 g/min; (×) IV = 1.0, Q = 6 g/min; (▲) IV = 0.75, Q = 6 g/min.

take-up velocity, but also exhibits a dependence on mass throughput and polymer molecular weight. Birefringence is increased by a decrease of mass throughput due to an increase in spinline stress that produces both higher orientation in the melt phase and higher resulting crystallinity due to increased stress induced crystallization. Because of the increase of orientation caused by oriented nucleation and growth processes during stress-induced crystallization, a substantial increase in orientation generally accompanies an increase of crystallinity.

As in the case of its effect on crystallinity described above, the effect of molecular weight is not as obvious as the effect of mass throughput. Increasing the molecular weight will lead to higher spinline stress. In the absence of other compensating effects this should lead to increased orientation. But because the development of crystallinity can be affected independently by molecular weight, there may be a reversal of the expected behavior. In the present case this effect apparently reduces the crystallinity developed (Fig. 3), which leads to lower overall orientation and birefringence. The very low birefringence of the low IV polymer when spun with a mass throughput of 6 g/min and a take-up velocity of less than 1500 m/min correlates with the low crystallinity of these filaments.

Comparing the birefringence results to the X-ray patterns of Figure 2, we observe that high crystalline orientations and high birefringences are developed at take-up velocities in the neighborhood of about 3500 m/min and above. These qualitative observations are presented in a more quantitative

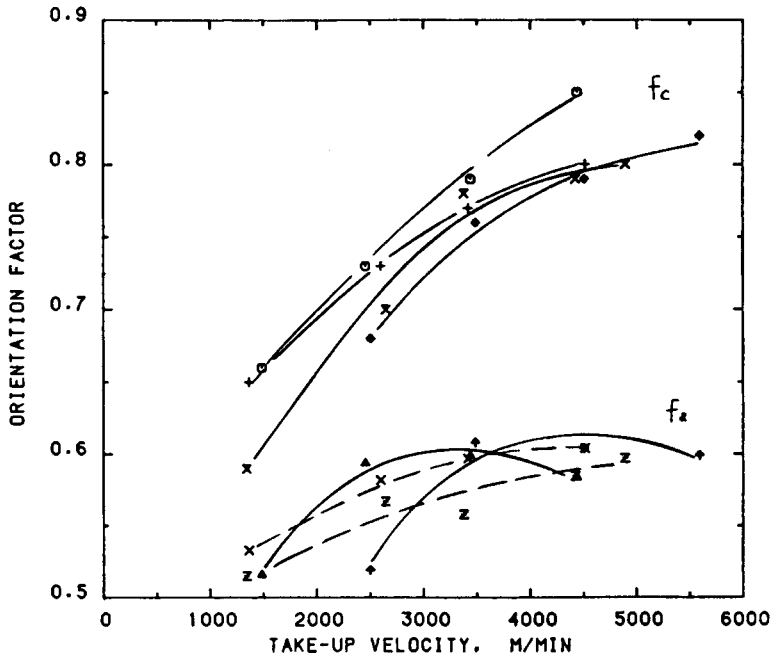


Fig. 10. Orientation factor vs. take-up velocity: (⊙) IV = 0.75, Q = 4 g/min; (◇) IV = 0.75, Q = 6 g/min; (×) IV = 1.0, Q = 6 g/min; +, IV = 1.0, Q = 4 g/min; (×) IV = 1.0, Q = 4 g/min; (Ƶ) IV = 1.0, Q = 6 g/min; (↑) IV = 0.75, Q = 6 g/min; (▲) IV = 0.75, Q = 4 g/min.

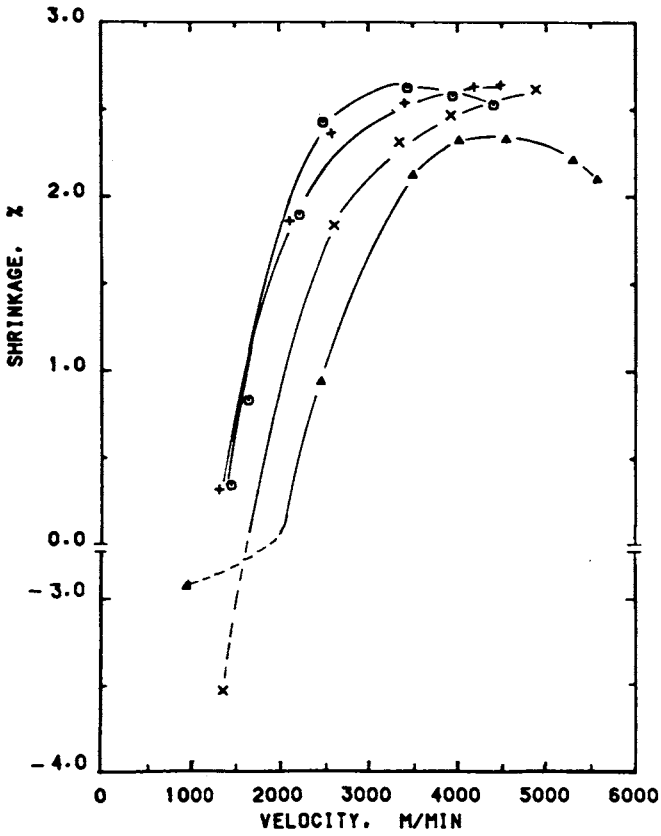


Fig. 11. Shrinkage (boiling water) as a function of take-up velocity: (⊙) IV = 0.75, Q = 4 g/min; (+) IV = 1.0, Q = 4 g/min; (×) IV = 1.0, Q = 6 g/min; (▲) IV = 0.75, Q = 6 g/min.

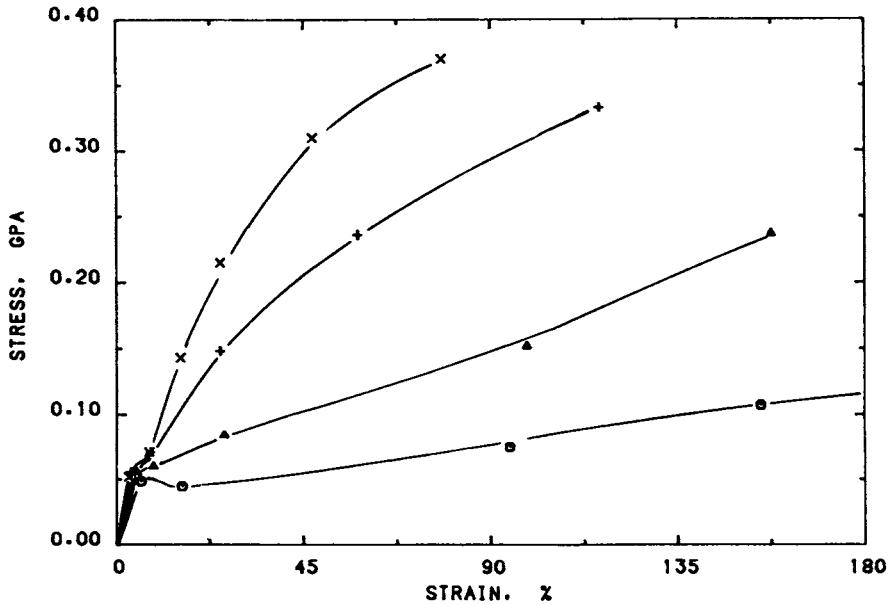


Fig. 12. Stress–strain curves of as-spun filaments with IV = 0.75, Q = 4 g/min at various take-up velocities: (⊙) 1500 m/min; (▲) 2500 m/min; (+) 3500 m/min; (×) 4500 m/min.

way in Figure 10, where the Hermans orientation factors are plotted vs. take-up velocity for both the crystalline and amorphous phases in the filaments. The crystalline orientation is always substantially higher than the amorphous orientation. The orientation of both phases generally increases with increasing take-up velocity, though there is evidence of a slight maximum in some of the amorphous phase data. Maxima have previously been reported in the amorphous phase orientation factors of PET filaments spun at high spinning speeds.[23-26]

## Shrinkage

The boiling water shrinkage of the filaments is shown in Figure 11. Conditions that produce filaments with low levels of crystallinity (high mass throughput and low spinning speeds) result in filaments that expand rather than shrink during the shrinkage test. Increase in take-up velocity results in shrinkage which increases until a saturation value or slight maximum is reached at a shrinkage value of about 2.5%. The rapid increase of shrinkage occurs at lower take-up velocities for samples spun at the lower mass throughput. At a given take-up velocity, the shrinkage seems to be related to the crystallinity and orientation values previously described. This is not surprising as shrinkage is expected to correlate with relaxation of the orientation in amorphous regions in samples containing appreciable orientation. In the present case a portion of the shrinkage may also be related to conversion of the $\beta$-form to $\alpha$-form during the shrinkage test, at least in those samples that contain some $\beta$-form initially.

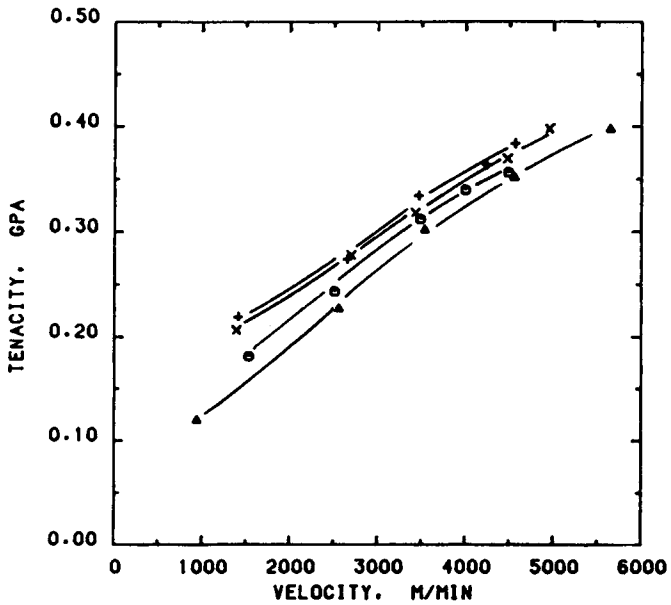


Fig. 13. Tenacity as a function of take-up velocity: (+) IV = 1.0, Q = 4 g/min; (×) IV = 1.0, Q = 6 g/min; (⊙) IV = 0.75, Q = 4 g/min; (▲) IV = 0.75, Q = 6 g/min.

The reason for the expansion at low crystallinity levels is not entirely clear, but it is perhaps related to penetration and swelling of the filament by the water followed by thermal crystallization. This effect is similar in nature and, perhaps, in origin to the growth of nylon 6 yarns during conditioning and equilibration with the environment following spinning at low spinning speeds.[27]

The shrinkage behavior of PBT is quite different from that reported for PET.[23,25,26,28] In the latter case the shrinkage is very high at low spinning speeds and decreases rapidly as take-up velocities reach levels where crystallization occurs on the spinline.

## Mechanical Properties

Figure 12 shows typical stress versus strain curves for filaments of the low IV polymer spun with different take-up velocities and a mass throughput of 4 g/min. The shape of the curves changes greatly with change of take-up velocity. Tenacity and initial modulus increase and elongation to break decreases as take-up velocity increases. Similar trends were observed for samples spun from the other polymer and at different mass throughput.

The variations in tenacity, modulus and elongation to break are shown for all samples in Figures 13, 14, and 15, respectively. These figures show that tenacity and modulus increase as both take-up velocity and molecular weight (IV) increase and as mass throughput decreases. Cross plots (not shown) of the tenacity and modulus as a function of crystallinity and birefringence indicate that both properties increase as orientation and crystallinity increase. In addition, there seems to be an incremental increase, especially in the case of the modulus, associated with increasing the molecular weight that is above that due to crystallinity and orientation alone.

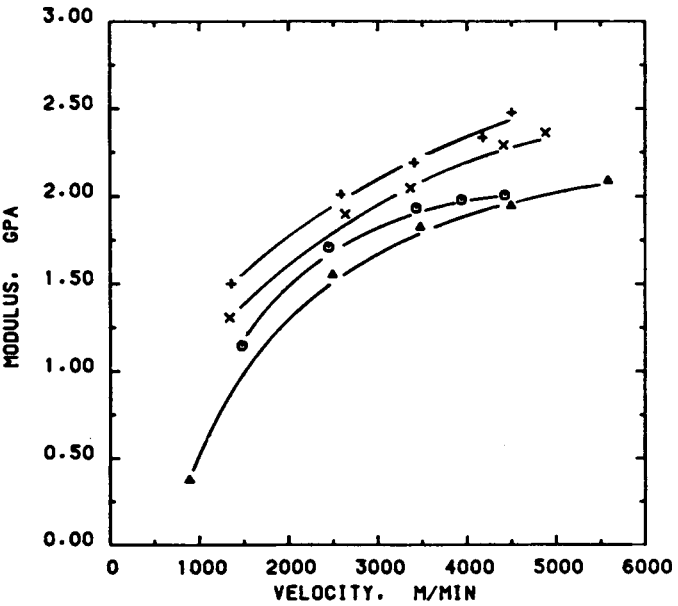


Fig. 14. Modulus as a function of take-up velocity: (+) IV = 1.0, Q = 4 g/min; (×) IV = 1.0, Q = 6 g/min; (⊙) IV = 0.75, Q = 4 g/min; (▲) IV = 0.75, Q = 6 g/min.

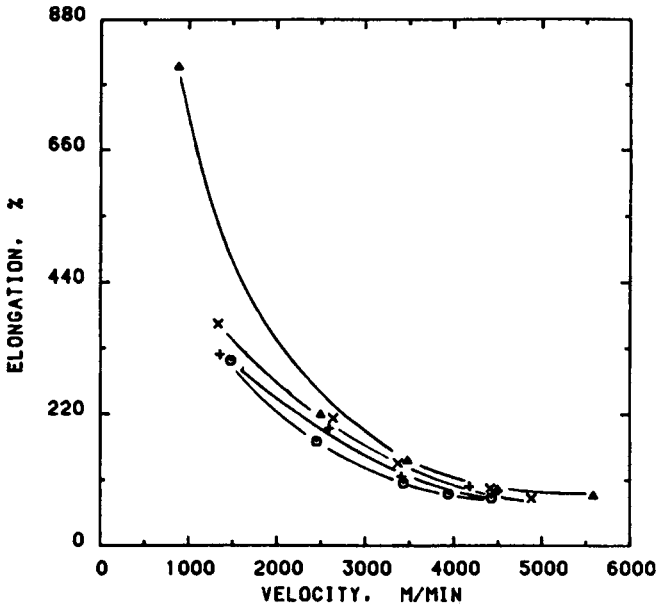


Fig. 15. Elongation as a function of take-up velocity: (▲) IV = 0.75, Q = 6 g/min; (×) IV = 1.0, Q = 6 g/min; (+) IV = 1.0, Q = 4 g/min; (⊙) IV = 0.75, Q = 4 g/min.

The initial portions of stress versus strain curves for selected filaments are shown on an expanded scale in Figure 16. Each of the curves shows a plateau region occurring at a stress in the range 0.05–0.07 GPa and strains of about 2.5–8.0%. It is well documented in the literature that PBT undergoes a phase transformation from $\alpha$-form to $\beta$-form during elongation of films or filaments

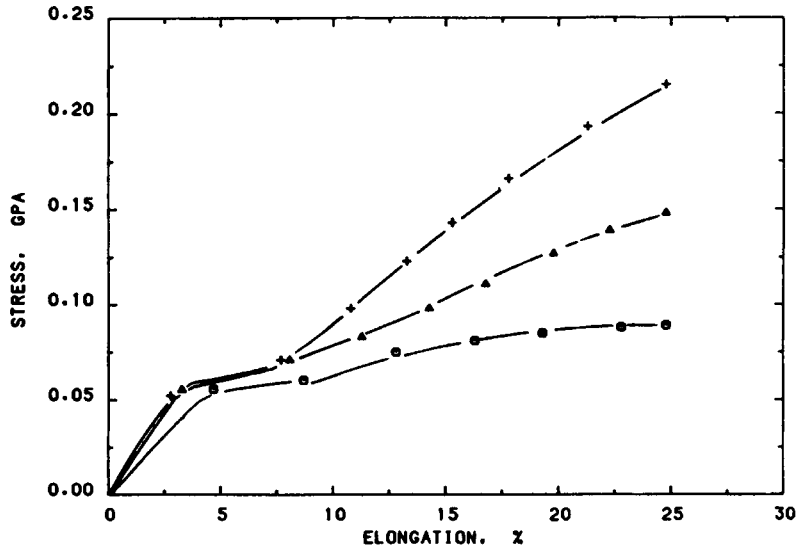


Fig. 16. Stress vs. elongation curves for as-spun filaments with IV = 0.75, Q = 4 g/min; enlargement of Figure 9: (⊙) take-up velocity 2500 m/min; (▲) take-up velocity 3500 m/min; (+) take-up velocity 4500 m/min.

that initially contain $\alpha$-form crystals. The observation of the plateau is further evidence that the as-spun filaments contain substantial quantities of $\alpha$-form crystals. It might be noted that samples that have very low crystallinities do not exhibit a similar plateau in their stress vs. strain curves, although they do exhibit yield points. The length of the plateau should correlate with the $\alpha$-form content present in the filament, and the present data appear to confirm this expectation. In addition, there is some indication from the stress vs. strain curves that filaments spun under the highest stresses contain some $\beta$-form content. However, because the amount of $\beta$-form is small, any such result may simply be fortuitous, and we choose not to pursue this further.

## SUMMARY AND CONCLUSIONS

The structure and properties of PBT filaments developed during melt spinning were found to vary over a wide range, and they were influenced by both molecular weight and spinning variables such as extrusion rate (mass throughput), take-up velocity, and cooling conditions. Amorphous (glassy) filaments were produced under conditions corresponding to relatively high cooling rates and low spinning speeds. For a given molecular weight polymer, the crystallinity, molecular orientation, and crystal size increased with an increase in take-up velocity or a reduction of the mass throughput, both factors that lead to increased spinline stress levels. This suggests that the structure developed is largely controlled by a balance between the spinline stress level achieved and the cooling conditions imposed.

The inherent crystallization kinetics of the polymer are also a key factor in determining the structure resulting from a given combination of spinning conditions. The crystallization kinetics of PBT are higher than those of PET, and the increase of crystallinity with increase of take-up velocity occurs at lower take-up velocities for PBT than for PET, other factors being equal. Changing the molecular weight has the potential for changing both the spinline stress (through a change in viscosity) and the inherent crystallization kinetics. Evidence was presented that both factors may be important in determining the structure of PBT filaments. The effect of increased viscosity produced by increasing the molecular weight leads to greater stress-induced crystallization rates for a given set of spinning conditions. However, under a given stress level, the inherent crystallization kinetics appear to decrease somewhat with increasing molecular weight. This factor tends to modify the effect of increased stress level, resulting in a lower crystallinity development than would be observed for a polymer of lower molecular weight spun under conditions that produce the same spinline stress.

The crystals in melt spun PBT filaments are largely of the $\alpha$-form. Evidence was found that a small amount of $\beta$-phase may be retained in PBT filaments spun under very high stress levels. It is not possible to determine from the present data whether $\alpha$-form or $\beta$-form crystallizes directly from the melt at low spinline stresses, but the presence of $\beta$-form in samples spun under high stresses suggests that some $\beta$-form may crystallize from the melt under these conditions.

The tenacity and tangent modulus increase and elongation to break decreases with increase of take-up velocity or decrease of mass throughput. These effects appear to reflect the changes in crystallinity and orientation

described above. Increasing the molecular weight also resulted in an increase of the modulus and tenacity, other factors remaining equal. There was some evidence that the increase of modulus was greater than that caused by the increase of orientation and crystallinity alone.

Above a take-up velocity of 2500 m/min the shape of the stress–strain curve changes; the characteristic plateau corresponding to the $\alpha$- to $\beta$-form crystal–crystal transformation was observed. The length of this plateau increased with increase of take-up velocity and the $\alpha$-form crystal content of the sample.

## References

1. C. A. Boye, Jr., and J. R. Overton, *Bull. Am. Phys. Soc.*, **19**, 352 (1974).
2. R. Jakeways, I. M. Ward, M. A. Wilding, J. H. Hall, I. J. Desborough, and M. G. Pass, *J. Polym. Sci., Polym. Phys. Ed.*, **13**, 799 (1975).
3. Z. Mencik, *J. Polym. Sci., Polym. Phys. Ed.*, **13**, 2173 (1975).
4. R. Jakeways, T. Smith, I. M. Ward, and M. A. Wilding, *J. Polym. Sci., Polym. Lett. Ed.*, **14**, 41 (1976).
5. M. Yokouchi, Y. Sakakibara, Y. Chatani, H. Tadokoro, T. Tanaka, and K. Yoda, *Macromolecules*, **9**, 266 (1976).
6. I. H. Hall and M. G. Pass, *Polymer*, **17**, 807 (1976).
7. M. G. Brereton, G. R. Davies, R. Jakeways, T. Smith, and I. M. Ward, *Polymer*, **19**, 17 (1978).
8. B. Stambaugh, J. L. Koenig, and J. B. Lando, *J. Polym. Sci., Polym. Phys. Ed.*, **17**, 1053 (1979).
9. I. M. Ward, M. A. Wilding, and H. Brody, *J. Polym. Sci., Polym. Phys. Ed.*, **14**, 263 (1976).
10. K. Tashiro, Y. Nakai, M. Kobayashi, and H. Tadokoro, *Macromolecules*, **13**, 137 (1980).
11. R. S. Stein and A. Misra, *J. Polym. Sci., Polym. Phys. Ed.*, **18**, 327 (1980).
12. Shude Rong and H. L. Williams, *J. Appl. Polym. Sci.*, **30**, 2575 (1985).
13. Fumin Lu and J. E. Spruiell, *J. Appl. Polym. Sci.*, **31**, 1595 (1986).
14. H. M. Heuvel, R. Huisman, and K. C. J. B. Lind, *J. Polym. Sci., Polym. Phys. Ed.*, **14**, 921 (1976).
15. G. Farrow and J. Bagley, *Text. Res. J.*, **32**, 587 (1962).
16. V. B. Gupta, *Text. Res. J.*, **49**, 405 (1979).
17. N. Yoshihara, A. Fukushima, Y. Watanabe, et al., *Sen-i Gakkaishi*, **37**(10), 387 (1981).
18. R. S. Stein and F. H. Norris, *J. Polym. Sci.*, **16**, 381 (1956).
19. J. Shimizu, N. Okui, A. Kaneko, and K. Toriumi, *Sen-i Gakkaishi*, **34**, T-64 (1978).
20. H. M. Heuvel and R. Huisman, *J. Appl. Polym. Sci.*, **22**, 2229 (1978).
21. J. Shimizu, N. Okui, T. Kitutani, and K. Toriumi, *Sen-i Gakkaishi*, **34**, T-93 (1978).
22. K. Koyama, J. Suryadevara, and J. E. Spruiell, *J. Appl. Polym. Sci.*, **31**, 2203 (1986).
23. G. Perez and C. Lecluse, "High Speed Spinning of Polyethylene Terephthalate by Pneumatic Take-up," in 18th Int. Man-Made Fiber Conference, Dornbirn, Austria, June 20–22, 1979.
24. A. Ziabicki, *Fiber World*, 8, (Sep.) 8 (1984).
25. G. Perez, in *High Speed Fiber Spinning*, A. Ziabicki and H. Kawai, Eds., Wiley, New York, p. 333.
26. G. Vassilatos, B. H. Knox, and H. R. E. Frankfort, in *High Speed Fiber Spinning*, A. Ziabicki and H. Kawai, Eds., Wiley, New York, p. 383.
27. J. Shimizu, *Sen-i Gakkaishi*, **38**, 499 (1982).
28. I. Jacob and H. R. Schroeder, *Chemiefasern*, **30**, 228 (1980).

Received July 15, 1986
Accepted July 17, 1986